Theoretical–experimental analysis of the heat transfer in a helical condenser for a heat transformer integrated to a water purification system

A.H. Hernández[a], O. Flores[a], A. Huicochea[b], A. Álvarez[b], F.Z. Sierra[b], S. Silva[b], J.A. Hernández[b],*

[a]_Posgrado en Ingeniería y Ciencias Aplicadas de la Universidad Autónoma del Estado de Morelos, Av. Universidad No. 1001, Col Chamilpa, CP. 62209 Cuernavaca, Morelos, Mexico, Tel. +52 01 777 3297084; emails: angel.hernandez@uaem.mx (A.H. Hernández), oliver.flores@uaem.mx (O. Flores)_
[b]_Centro de Investigación en Ingeniería y Ciencias Aplicadas (CIICAp), Universidad Autónoma del Estado de Morelos (UAEM), Av. Universidad No. 1001, Col Chamilpa, CP. 62209 Cuernavaca, Morelos, Mexico, Tel. +52 01 777 3297084; emails: huico_chea@uaem.mx (A. Huicochea), aalvarez@uaem.mx (A. Álvarez), fse@uaem.mx (F.Z. Sierra), ssilva@uaem.mx (S. Silva), alfredo@uaem.mx (J.A. Hernández)_

ABSTRACT

A theoretical–experimental analysis was carried out to acquire the coefficient of condensation heat transfer in a double-helical tube coupled to an absorption heat transformer, the last one operating with two working solutions (water and Carrol-water). In the condenser, the steam flows through the inner tube and the cooling water flows in countercurrent in the annular section. The condenser pressure is located within the ranges from 3.7 to 9.2 kPa with a Reynolds number of steam ranging from 6,400 to 23,500 for water and 6.1 to 9.2 kPa with a Reynolds number of steam ranging from 5,550 and 22,000 for the Carrol-water. The mass flux of the cooling water ranges from 450 to 850 kg/m^{2}s and 750 to 1,050 kg/m^{2}s, respectively. Two methods are used for calculating the condensation heat transfer coefficient: the first considers the energy balance and heat transfer equations; and the second is by Wilson plot technique. The heat transfer coefficient results show similarity between both methods and ranges from 2,400 W/m^2°C ≤ α_{con} ≤ 6,100 W/m^2°C and 810 W/m^2°C ≤ α_{con} ≤ 5,650 W/m^2°C, respectively. In addition, a mathematical model is applied using condensation coefficients obtained in the theoretical and experimental analysis. This model is given by algebraic and differential equations, obtaining satisfactory results in the energy flows. The equations were selected according to the phases and regime of the fluid to be condensed. Also a correlation for the condensation heat transfer coefficient based on the Nusselt, Reynolds, and Prandtl numbers for each of the two solutions is proposed. Finally, in the absorption heat transformer considering Carrol-water as a working fluid, it was possible to generate pure water in the water purification system.

Keywords: Mathematical model of simple cell; Nusselt number; Carrol-water

*Corresponding author.

1. Introduction

Helical heat exchangers are widely used due to its compact size and a higher rate of heat transfer compared to heat exchangers straight tube. They are used in solar collectors, air conditioning, nuclear power systems, cooling, systems development, and waste heat recovery [1]. Examples of heat recovery systems are heat transformers (by absorption heat pumps); these devices raise the temperature of a source of low energy to a higher level [2,3]. The heat obtained can be used in residential, commercial, and industrial; for example, in process of heating, cooling, and purification of effluents, etc. [4].

Fig. 1 describes the process of heat transformer which consists of five heat exchangers. In this system, two fluids circulate as heat energy which is transferred without mixing, internal circuit of the generator runs Carrol-water, on the outside heat is supplied (14). This heat vaporizes the working fluid part (7) which flows to the condenser; the working fluid is condensed by giving up heat to an external source (13). The working fluid in liquid phase (8) is pumped to the evaporator (9) and changes to the vapor phase component (10), due to external heat supply (12). The generated steam is mixed with the concentrated solution (1) from the generator; that is pumped through the economizer (2), (3) to the absorber, where the result of this mixture is an exothermic reaction, whose energy (11) is used for water purification. The resulting mixture is diluted solution (4) pumped through the economizer (5) toward the generator (6) to restart the cycle.

The main components of a heat transformer for a refining cycle are: an evaporator, an absorber, a generator, an economizer, and a condenser [5]. The purpose of the condenser is to change the vapor phase to the liquid phase by some type of cooling fluid, in this case water. Convective heat transfer coefficients take a very important role in the design, manufacture, and performance of heat exchange equipment; and for modeling and simulation of processes. To achieve a better efficiency in heat transfer would have to focus on miniaturization as well as on the increased heat flow, which would reduce the total thermal resistance and would promote a superior heat transfer convective coefficient [6].
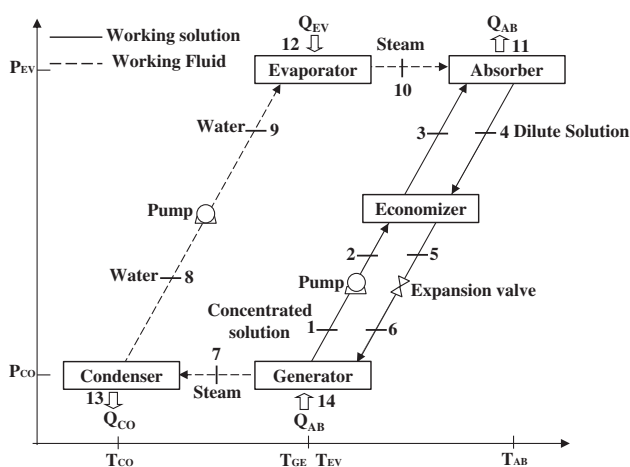
Colorado et al. [7], and Colorado-Garrido et al. [8] proposed a model to predict promptly (from control volumes) momentum and energy transfer for the condenser and evaporator system of absorption heat transformer. The authors used heat transfer coefficients reported in the literature with results of 10–20% error.

Dalkilic and Wongwises [9,10], Laohalertdecha et al. [11], and Balcilar et al. [12] conducted a review on the studies of condensation on smooth tubes in the section of phase change, which is the most complicated to study on heat exchange systems. Investigations were classified according to the orientation of the tube and its geometry. The fall of pressure, flow pattern, void fraction, and characteristics of the different refrigerants used were obtained from the literature.

Xin et al. [13] studied the pressure drop in the single-phase and two-phase region in the annular section of horizontal and vertical helical pipes with air–water flow. The experiments showed a range of Reynolds number from 210 to 23,000 for water, and a range of 30 to 30,000 for air. A friction factor correlation for single-phase flow in laminar, transition, and turbulent flow regime was proposed. The variation of pressure drop in two-phase region depends on the parameter of Lockhart–Martinelli, as well as the rate of flow of air or water. The effect of flow velocity tended to diminish as the tube diameter decreased.

Kang et al. [14] investigated the heat transfer and pressure drop in the condensation of HFC-134a, flowing through a helical tube of 12.7 mm internal diameter of the inner tube. Experiments on a range of mass flow rate from 100 to 400 kg/m²/s of the refrigerant, the Reynolds number of the cooling water is in a range from 1,500 to 9,000 at a fixed temperature of 33℃, and the temperature of the tube wall is in the range of 12–22℃. The single-phase flow and vapor–liquid flow coexist in the helical tube. The effects of tube wall temperature on the heat transfer coefficients and pressure drops were investigated. The results showed that side of the refrigerant heat transfer coefficients decrease with increasing mass flux or the

Fig. 1. Thermodynamic cycle of heat transformer.

cooling water flow Reynolds number. The authors proposed and compared to the correlations obtained from the measurement data with the straight tubes.

Rennie and Raghavan [15] conducted an experimental study on coil heat exchangers using two different geometries. Both exchangers were subjected to configurations in parallel and counter flow. Heating and cooling water was used as a working fluid. Overall heat transfer coefficients were determined and the convective coefficients for inner tube and the annulus were calculated using the method Wilson plot. Nusselt numbers for both sides of the heat exchanger were obtained and were compared with those reported in the literature.

Singh et al. [16] presented a study of condensing heat transfer for heat exchangers with finned tubes at different pressures between 100 and 200 kPa, by varying the flow in the cooling system of 8 (Re ≈ 12,000) to 16 lpm (Re ≈ 24,000). The condensation transfer coefficient was calculated using the Wilson plot method. Correlations were developed to calculate the heat transfer coefficient for horizontal arrays of n-finned tubes.

Kumar et al. [17] conducted an experimental study of water vapor condensation and the refrigerant R-134a on the outside of horizontal tubes and fin tubes. The experimental coefficient of heat transfer based on direct measurement of the temperature of the tube wall was compared with that predicted by the Wilson plot method. The heat transfer coefficient of underestimate steam ranged from 7.5 to 15% difference between the two methods and the R-134a underestimate refrigerant ranged between 13 and 25%.

In this work, the first objective is to calculate the condensation heat transfer coefficient, through experimental measurements for two work solutions (water and Carrol-water) by two different systematic: the first makes use of a thermodynamic algorithm; the second applies the Wilson plot methodology for systems in stable condition. The second objective is the estimation of the purified water when working with Carrol-water and their relation with the condensation heat transfer coefficient. Finally, the third objective is to use the estimated results (Nu, Re, Pr, α) to illustrate the dynamics of the heat exchanger using a finite differential equations of first-order model and to propose a correlation to estimate the condensation heat transfer coefficient.

2. Experimental data

To obtain the heat transfer coefficients, temperature, flow, and pressure of the condenser experimental tests were carried out in the heat transformer.

This device is attached to a water purification system, the transformer was used in real conditions of operation of the complete thermodynamic cycle (generation, condensation evaporation and absorption), using two working solutions: water and Carrol-water. In this equipment, the water to purify may come from different sources as water contaminated or sea water. Fig. 2 shows the experimental equipment.

2.1. Steam generation

Hot water as power supply to the steam generator was used for the generation of steam. The water comes from a tank heated by electric resistances which regulates the temperature of the water inside the tank. Once water flows through the steam generator to transfer their energy it returns to the container. There is generation of steam when the water inside the generator reaches saturation temperature. The saturation temperature is based on the pressure (Eq. (1)):

$$T_{sat} = f(P) \tag{1}$$

The condenser is a helical double-pipe. Through the inner tube flows steam from the generator to be condensed and in the annular section flows water
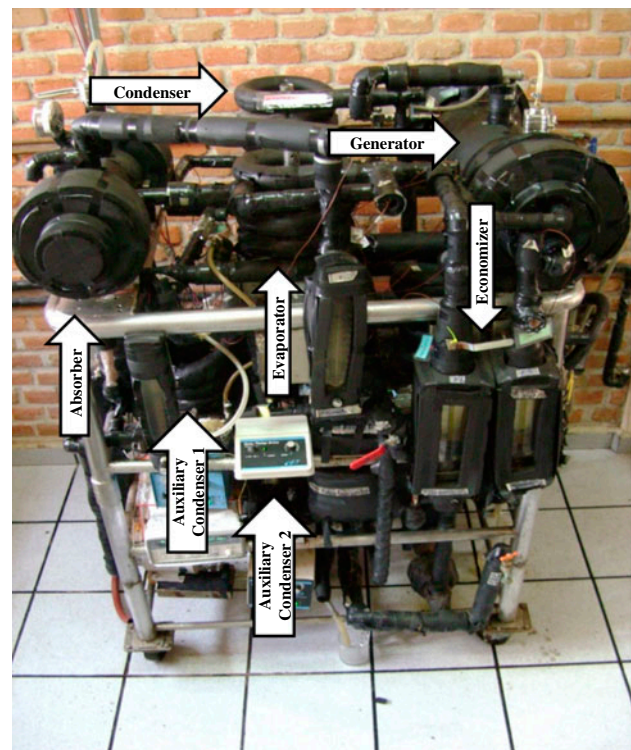
Fig. 2. Experimental equipment.

from cooling tower. Cooling systems are required to remove the heat; these typically consist of a cooling tower whose heat exchangers are in a settlement against the current.

Manufacturing material is stainless steel 316L.

Fig. 3 shows the schematic diagram of the condenser. Table 1 describes the dimensions of helical condenser. A detailed schematic of the thermal processor is shown in Fig. 4.

When the working solution was water, experiment consisted to vary the flow of cooling water in the range of 450–850 kg/m² s regulated by a manually operated valve. This procedure was carried out in the range of 3.8–9.1 kPa pressure. For the Carrol-water solution, the range of variation of the cooling flow was 750–1,050 kg/m² s with a range of 7.1–9.3 kPa pressure.

2.2. Instrumentation, measurement, and data acquisition

Cooling water flow measurement was performed using a flowmeter for measuring range: 1.5–15 l/min. The accuracy of the flowmeter is ±3% on the measurement of the total scale.

For measuring the temperature, type T thermocouples were calibrated with a reference thermometer (±0.1°C) resulting with an uncertainty of ±0.2°C used for each thermocouple. To measure the pressure, a pressure transducer was used with a measuring range −101.35 to 103.42 kPa and with an accuracy of ±0.25% of full scale.

A data acquisition system from Agilent Technologies 34970A series with an HP 34901A multiplexer module with 20 input channels for direct voltage measurement thermocouples and pressure transducer was used.
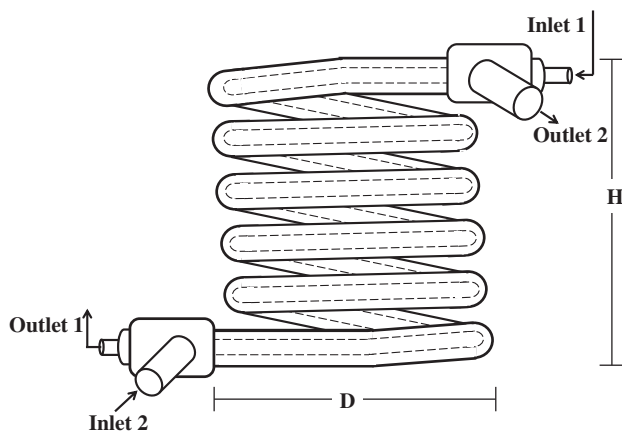
Fig. 3. Experimental helical double-pipe condenser used in the absorber heat transformer.

Since the start of the experiment, data are recorded every 10 s, the condenser goes through a transitional state until it manages to reach a stable state. Table 2 shows the changes in the mass flux. Table 3 presents the conditions of operation for each of the tests.

3. Theoretical analysis

A thermodynamic model was developed to estimate the condensation coefficient of water vapor. The thermodynamic properties of water were calculated according to [18]. Considerations for the estimation of the coefficient of heat transfer in the condenser are as follows:

(1) The analysis is performed under steady-state conditions.
(2) The fall of pressure in the pipes is negligible.
(3) The condition of steam entering the condenser is saturated and liquid sub-cooling at exit.
(4) The loss of heat to the environment in the condenser is negligible.

3.1. Energy balance and heat transfer equations

The power of the condenser is calculated by the temperature difference of the external heating water flow:

$$Q_{co} = \dot{m}_{ext} C p_{ext} (T_{out} - T_{in})_{ext} \tag{2}$$

The mass flow of steam that condenses on the inside of the tube is calculated from the energy balance with respect to the enthalpies of the steam at the entrance and the exit of the condenser.

$$\dot{m}_v = \frac{\dot{Q}_{co}}{h_{v,in} - h_{ls,out}} \tag{3}$$

According to the consideration Eq. (3) we have:

$$h_{v,in} = f(P_{co}) \tag{4}$$

$$h_{ls,out} = f(T_{se}, P_{co}) \tag{5}$$

The power of the condenser is the sum of the power required for the phase change $\dot{Q}_{cf}$ and the sub-cooling condensate $\dot{Q}_{se}$ mathematically expressed with the following equation:

$$\dot{Q}_{co} = \dot{Q}_{cf} + \dot{Q}_{se} \tag{6}$$

Table 1
Dimensions of the helical double-pipe condenser

	Internal pipe (mm)	External pipe (mm)
External diameter	9.52	19.05
Internal diameter	6.22	15.75
Helical diameter	240	240
Turns	4	4
Length	3,500	3,500
Height	300	300

The power required for the phase change in saturation conditions is:

$$\dot{Q}_{cf} = \dot{m}_v (h_v - h_l)_{sat} \tag{7}$$

The power required for the sub-cooling is calculated from the balance of power with Eq. (6):

$$\dot{Q}_{se} = \dot{Q}_c - \dot{Q}_{cf}$$
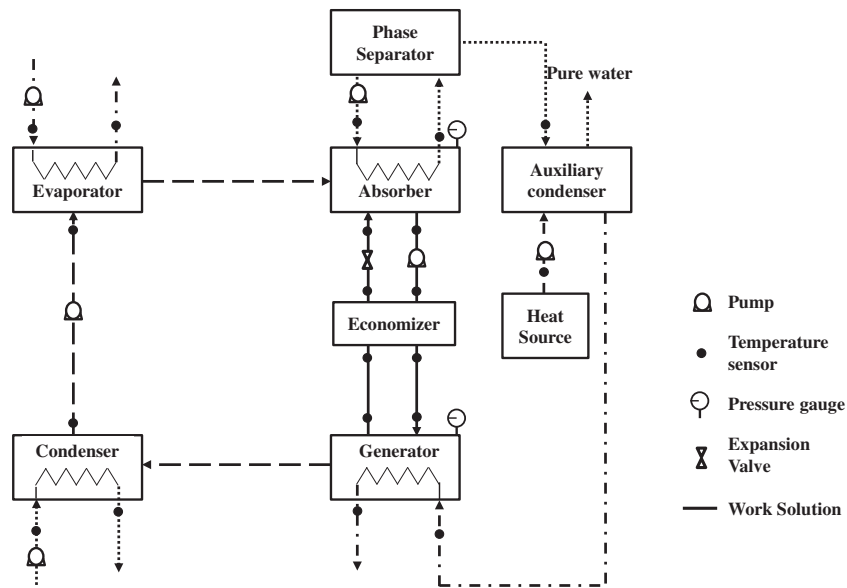
Fig. 4. Detailed schematic diagram of heat transformer.

Table 2
Experimental design

Test	Water		Carrol-water	
	Mass flux (kg/m² s)	Pressure (kPa)	Mass flux (kg/m² s)	Pressure (kPa)
1	850	$3.70 \leq P \leq 4.47$	1,050	$6.13 \leq P \leq 6.35$
	666	$4.47 \leq P \leq 5.24$	950	$6.35 \leq P \leq 6.57$
	533	$5.24 \leq P \leq 6.01$	850	$6.57 \leq P \leq 6.79$
	450	$6.01 \leq P \leq 6.80$	750	$6.79 \leq P \leq 7.0$
2	850	$7.84 \leq P \leq 8.17$	1,050	$7.1 \leq P \leq 7.64$
	666	$8.17 \leq P \leq 8.50$	950	$7.64 \leq P \leq 8.18$
	533	$8.50 \leq P \leq 8.84$	850	$8.18 \leq P \leq 8.72$
	450	$8.84 \leq P \leq 9.2$	750	$8.72 \leq P \leq 9.25$

Table 3
Operating conditions

Test		Wáter					Carrol-wáter				
		P (kPa)	$(T_{in})_{int}$ (°C)	$(T_{out})_{int}$ (°C)	$(T_{in})_{ext}$ (°C)	$(T_{out})_{ext}$ (°C)	P (kPa)	$(T_{in})_{int}$ (°C)	$(T_{out})_{int}$ (°C)	$(T_{in})_{ext}$ (°C)	$(T_{out})_{ext}$ (°C)
1	Min	3.70	29.1	19.2	17.0	20.6	6.13	64.5	24.47	21.0	22.54
	Max	6.80	37.9	23.5	17.6	24.7	7.0	66	26.51	23.30	27.31
2	Min	7.84	40.2	23.5	17.6	24.7	7.10	57.6	20.10	16.36	17.83
	Max	9.20	42.6	28.2	19.3	28.1	9.25	66	22.6	19.95	25.93

In the section of sub-cooling fluid in terms of saturation decreases its temperature below the saturation temperature until you reach the exit of the condenser.

The equation of heat transfer in the section of phase is:

$$\dot{Q}_{cf} = (UA)_{cf}(LMTD)_{cf} \tag{8}$$

where $(UA)_{cf}$ is the multiplication of the overall heat transfer coefficient by the transfer area in the change phase section.

The difference of the logarithmic mean temperature in the section of phase change $(LMTD)_{cf}$ is defined as:

$$(LMTD)_{cf} = \frac{(T_{sat} - T_{out,ext}) - (T_{sat} - T_{turn,ext})}{\ln\left(\frac{T_{sat} - T_{out,ext}}{T_{sat} - T_{turn,ext}}\right)} \tag{9}$$

where $T_{turn,ext}$ is the temperature of the cooling water in which the internal flow is located in saturated liquid phase. This temperature is calculated by means of a power balance using the following equation:

$$\dot{Q}_{se} = \dot{m}_{ext}Cp_{ext}(T_{turn} - T_{in})_{ext} \tag{10}$$

The overall thermal resistance of the section of phase change heat transfer is:

$$Rov = \frac{1}{(UA)_{cf}} = \frac{(LMTD)_{cf}}{Q_{cf}} \tag{11}$$

Condensation heat transfer coefficient (α_{con}) is calculated from the overall coefficient of heat transfer in the section of phase change (U_{cf}), the convective coefficient on the side of the cooling water (α_{ext}), and the resistance of heat transfer due to the wall of the inner tube (R_{wall}); considering that the fouling resistance is negligible, there is the following equation:

$$\alpha_{con} = \frac{1}{\frac{1}{U_{cf}} - \frac{1}{\alpha_{ext}} - R_w} \tag{12}$$

Table 4 presents the calculated values of the coefficient of evaporation (α_{con}).

3.2. Heat transfer coefficient by Wilson plot method

The overall thermal resistance can be expressed as the sum of resistances to heat transfer as:

$$Rov = R_{int} + R_w + R_{ext} \tag{13}$$

where the internal resistance is calculated using the following equation:

$$R_{int} = \frac{1}{\alpha_{int}A_{int}} \tag{14}$$

The resistance of the wall is calculated with the following equation:

$$R_w = \frac{\ln\left(\frac{r_{ext}}{r_{int}}\right)}{2\pi\lambda_{wall}L} \tag{15}$$

External resistance is calculated using the following equation:

$$R_{ext} = \frac{1}{\alpha_{ext}A_{ext}} \tag{16}$$

The elements taken as constants are grouped into the following equation:

$$C_1 = R_{ext} + R_w \tag{17}$$

The variation of the external convective coefficient is a function of speed; this variation can be represented by the following equation:

$$\alpha_{ext} = C_2 v_{ext}^m \tag{18}$$

where the coefficient m is assigned a value of 0.82 [19] (Dittus–Boelter) and C_2 is a constant with a value to be determined.

Finally, the overall thermal resistance obtained from experimental tests can be represented as a linear function of the experimental values of $1/V_{ext}^{0.8}$:

$$Rov = C_1 + \frac{1}{C - 2A_{ext}} \frac{1}{V_{ext}^m} \tag{19}$$

The coefficient of heat transfer of condensation on the inside of the condenser is calculated by combining Eqs. (14) and (17):

$$\alpha_{con} = \frac{1}{(C_1 - R_w)A_{int}} \tag{20}$$

A_{int} represents the heat transfer area in contact with the steam in the section of phase change.

Table 4
Results of the balances of mass, energy, and heat transfer for the condenser

Test		Wáter								Carrol-wáter							
		ΔT_{ext} (°C)	$\dot{Q}$(W)	$\dot{m}_v$ (kg/s) (1e−004)	α_{ext} (W/m²°C)	Re_v	α_{con} (W/m²°C)	Nu_v	U (W/m²°C)	ΔT_{ext} (°C)	$\dot{Q}$(W)	$\dot{m}_v$ (kg/s) (1e−004)	α_{ext} (W/m²°C)	Re_v	α_{con} (W/m²°C)	Nu_v	U (W/m²°C)
1	Min	2.60	767	3.10	1,713	6,386	2,400	518	599	1.45	792	3.28	12,493	5,346	811	323	546
	Max	7.0	2,053	8.29	3,060	16,548	4,556	1,519	1,278	4.16	2,264	9.40	13,032	15,330	5,270	1,511	1,818
2	Min	7.2	2,121	8.62	3,097	16,990	4,660	1,560	1,290	1.40	757	3.14	11,750	5,127	984	560	340
	Max	10.5	2,961	11.9	3,429	23,516	6,082	1,920	1,468	6.03	3,235	13.50	12,673	22,026	5,650	1,548	1,836
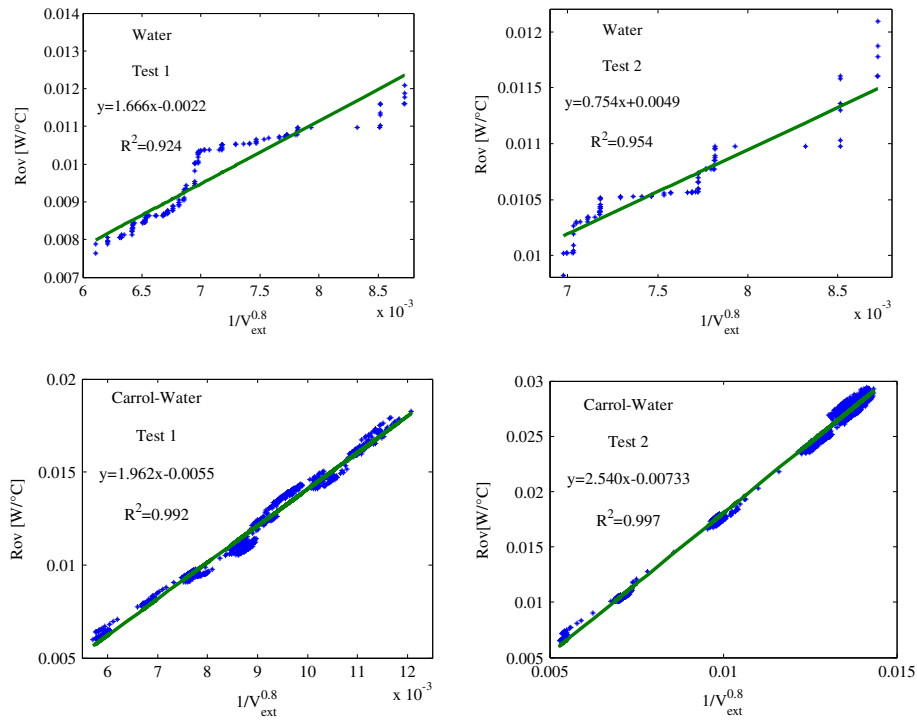
Fig. 5. Representation of overall thermal resistance based on the inverse of speed.
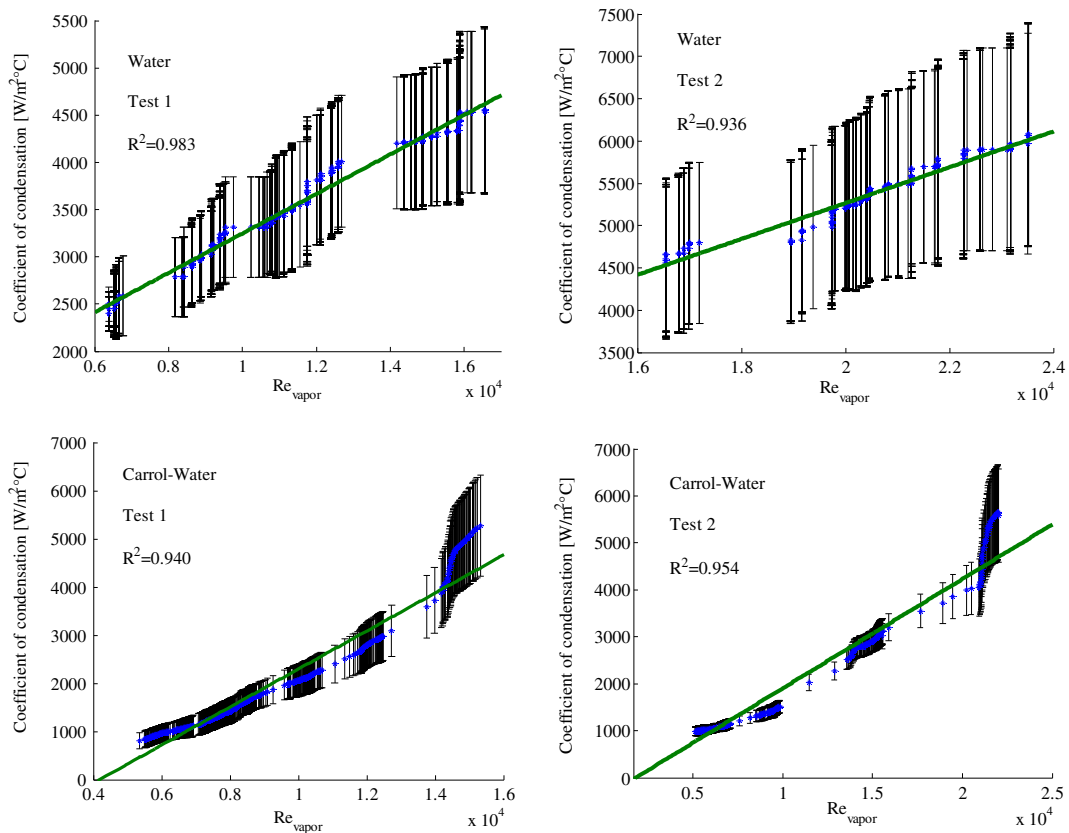
Fig. 6. Error associated with measurements.
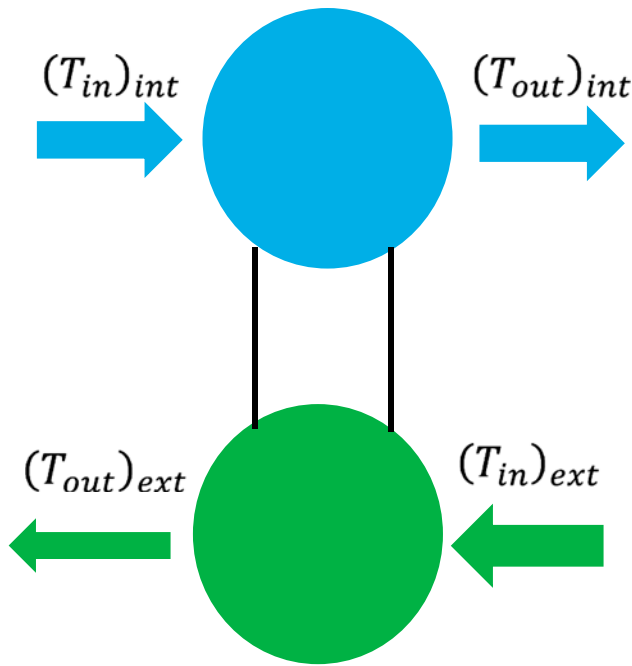
Fig. 7. Single-cell model.

Fig. 5 shows the calculated Rov values experimentally with respect to $1/V_{ext}^{0.8}$ used for the calculation of α_{con} using the method Wilson.

4. Uncertainty analysis

Fig. 6 presents values of the coefficient of condensation obtained from the energy balance using Eq. (20) for each of the tests, which include the error associated with the measurements.

The uncertainty for the steam condensation coefficient was calculated through the Taylor series method. Where, it is given by the model $y = f(x_1, x_2, \ldots, x_n)$, therefore the combined uncertainty is given by the following equation:

$$U_c^2(y) = \sum_{i=1}^{N} \left(\frac{\partial f}{\partial x_i} \right) u^2(x_i) \tag{21}$$

The uncertainty in the calculation of the transfer coefficient condensation due to the spread of the measurements is in the range of ±20 to ±25%.
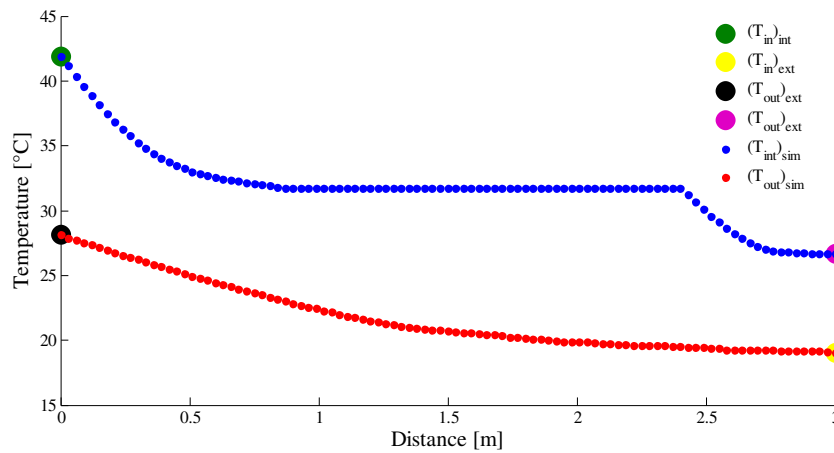
Fig. 8. Temperature profile of the coil condenser at a nominal operating point taken from the water test 2.

Table 5
Convective evaporation coefficient calculated by energy balances and Wilson plot method

	Wáter				Carrol-Wáter			
Test	$\dot{Q}(W)$	Re_v	$\alpha_{con,be}$ $(W/m^{2\circ}C)$	$\alpha_{con,wp}$ $(W/m^{2\circ}C)$	$\dot{Q}(W)$	Re_v	$\alpha_{con,be}$ $(W/m^{2\circ}C)$	$\alpha_{con,wp}$ $(W/m^{2\circ}C)$
1	1,420	11,550	2,630	3,060	1,080	8,760	1,820	2,050
2	2,530	20,210	3,260	3,570	1,100	8,700	1,060	1,240
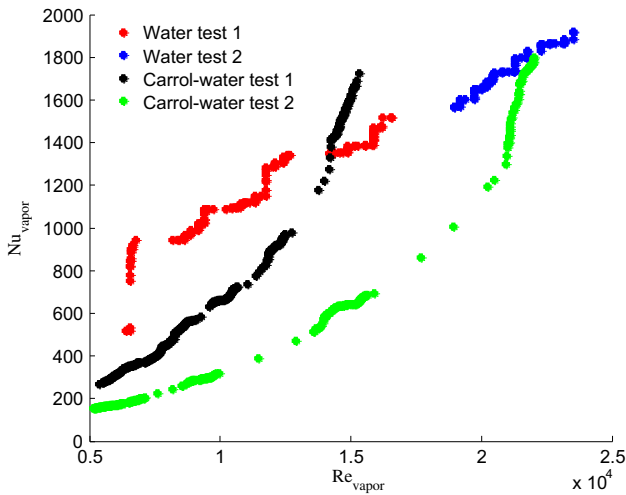
Fig. 9. Nusselt vs. Reynolds numbers for all tests in the condenser of the heat transformer.

Garcia Valladares [20] reported different coefficients of heat transfer of different refrigerants inside smooth tubes of between ±5 and ±30%.

5. Dynamics of the evaporator

The dynamics of the heat exchanger was obtained through differential equations of first order [21], given in Eq. (22):

$$
\begin{aligned}
\frac{dT_{int}}{dt} &= \frac{\dot{w}_{int}}{v_{int}}\left((T_{in})_{int}(t) - (T_{out})_{int}(t)\right) \\
&+ \left(\frac{\alpha_{cond}A_{int}}{Cp_{int}\rho_{int}V_{int}}\right)\left((T_{out})_{ext}(t) - (T_{out})_{int}(t)\right) \\
\frac{dT_{ext}}{dt} &= \frac{\dot{w}_{ext}}{v_{ext}}\left((T_{in})_{ext}(t) - (T_{out})_{ext}(t)\right) \\
&+ \left(\frac{\alpha_{ext}A_{ext}}{Cp_{ext}\rho_{ext}V_{ext}}\right)\left((T_{out})_{int}(t) - (T_{out})_{ext}(t)\right)
\end{aligned}
\tag{22}
$$

The works of [21] and [22] proposed to use the mathematical model described in Eq. (22), considering the parameter U according to the operating conditions of the system and the physical properties (ρ and Cp). Fig. 7 describes the model illustrated as a single cell, consisting of two perfectly stirred tanks with inflows and outflows [23], which is sufficient to estimate accurate states, without needing a larger number of cells as proposed by [24]. The calculated parameters energy balances are used in the mathematical model, which takes into account the following assumptions:

(1) The volume of water in the tube and annular section are constant.
(2) The heat transfer coefficient U is dependent on the flow and temperature of each fluid, and it is not considered as constant.
(3) There is no transfer of heat between the outer tube and the environment.
(4) The physical properties of water are evaluated depending on the temperature and pressure by means of empirical correlations.
(5) There is no energy storage in the walls of the tube.
(6) The inputs to the system are measurable; $(T_{in})_{int}$ and $(T_{in})_{ext}$.

Fig. 8 shows the obtained temperature profile mathematical model of the coil condenser at a nominal operating point of the test.

6. Results and discussion

Table 5 presents the comparison of the obtained condensation coefficient by means of energy balances calculated by the method Wilson plot. The difference in the heat transfer coefficient by these two techniques is primarily due to difference in the determination of test-section tube wall temperature by these two techniques. The Wilson plot technique underpredicts the condensing-side heat transfer coefficient by 7.5–15% for finned tubes and plain tubes, as well for condensation of steam. This is in agreement with the findings of [25] and [17] shows that for condensation of R-12 and R-134a, the Wilson plot underpredicts the heat transfer coefficient by 13–18% for condensation on a plain tube. In addition, the error of adjustment in the straight line for Wilson plots is obtained. The average values of the convection coefficients depend on the obtained condensate in the experimental tests carried out for both working solutions (water and Carrol-water). Condensate range: $3.10e{-}4 \geq \dot{m}_v \geq 11.9e{-}4$ and $3.28e{-}4 \geq \dot{m}_v \geq 13.50e{-}4$, respectively. The condensation coefficient calculated by Wilson plot underestimates between 9 and 17% calculated on the energy balance, which was a very useful tool in the analysis of complex configurations since it gives the possibility of including various factors, such as the numbers of tubes, the corrugations, and the change of phase with a limited number of measurements in solution.

Fig. 9 describes the Nusselt number for each value of Reynolds in the experimental tests performed at different operating conditions (heat flow and pressure). In the figure, we can observe a positive steam production for each of the tests performed. The

Table 6
Constants of the correlation Nusselt number for each test

Test	Graphic	C	m	n	R^2
Water					
1		0.0088	0.7037	1.9875	0.9516
2		0.0387	0.6709	1.0875	0.9540
Carrol-water					
1		1.975e–5	1.8914	1.8322	0.9895
2		6.294e–6	1.938	2.432	0.982
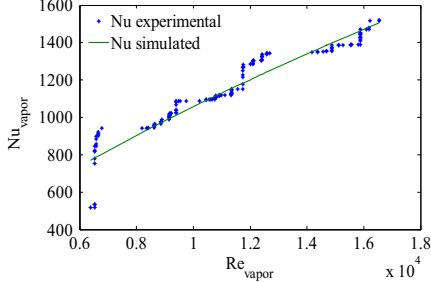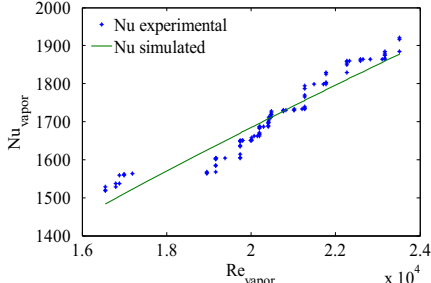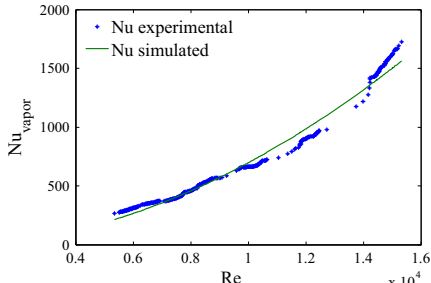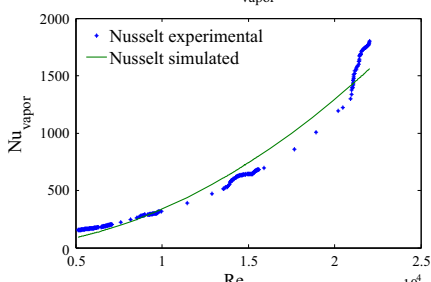
behavior is what differentiates the work solutions; increasing the pressure, caused by variations in the flow of cooling, giving rise to the heat transfer rate which will increase. The slope for Carrol-water increased in comparison to water slope, thus favoring the heat transfer rate. Now, if flow cooling decreases ΔT augments causing an increased steam generated at one higher rate, and may reach a point where the steam is formed more quickly than removed and the surface is covered with an insulating blanket of steam. This is film boiling. There is a value of ΔT where the coefficient was at a maximum and this dependence on the ΔT in transfer of evaporation coefficient has been reported frequently. Taking into account the nature of

Table 7
Reported literature vs. proposed correlation comparison

Carrol-water

Empirical correlation: Colorado et al. [7]　　　　　　　　　　　　　　　　　Empirical correlations: current

$$\text{Nu} = 0.023\,\text{Re}^{0.8}\,\text{Pr}^{0.4}\left[\text{Re}\left(\tfrac{d}{D}\right)^2\right]^{0.1}\left[1 + 4.863\left(-\ln\left(p_{\text{red}}\right)\tfrac{xg}{1-xg}\right)^{0.836}\right]$$

Test 1: $1.975\text{e} - 5\left(\text{Re}^{1.8914}\right)\left(\text{Pr}^{1.8322}\right)$
Test 2: $6.294\text{e} - 6\left(\text{Re}^{1.9360}\right)\left(\text{Pr}^{2.4320}\right)$
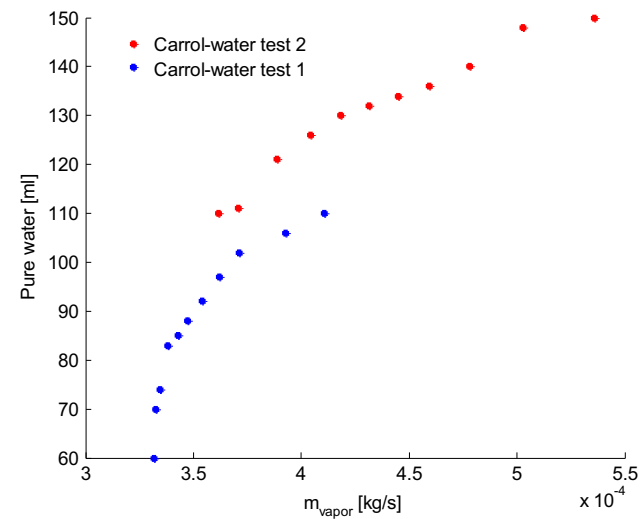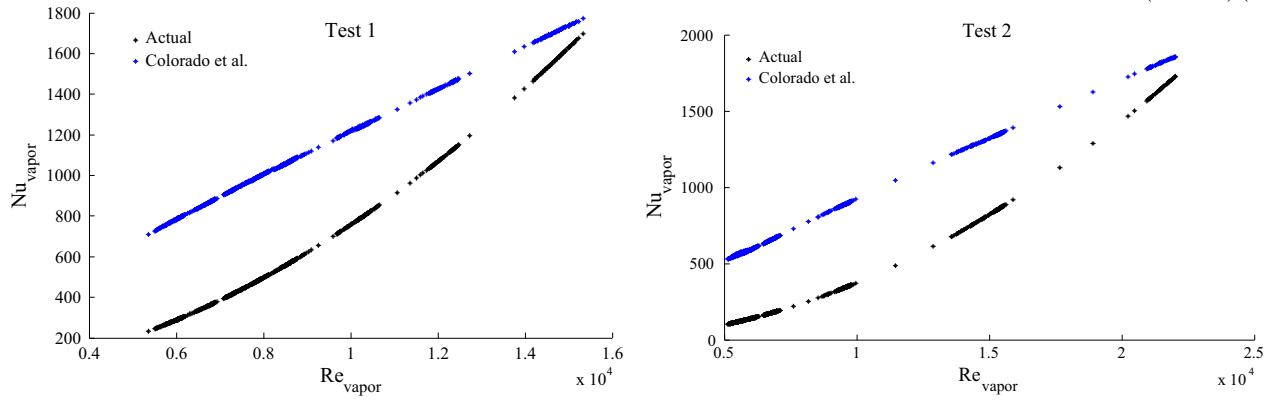
Fig. 10. Relationship of the condensed steam and purified water.

the two phases of the heat transfer in evaporation, one might also expect effects of factors such as surface tension vapor specific gravity and vapor mass ratio [26].

6.1. Construction of correlation semi-empirical Nusselt type for the calculation of the condensation coefficient

The problem of heat transfer by forced convection in a tube with fully developed laminar flow can be solved to some certain boundary conditions. When working with turbulent flow, systems with large variations in fluid properties, or with passages of non-circular geometries, the thickness of the boundary layer is normally difficult to determine from microscopic considerations. Hence, the analytical determination of the coefficient of heat transfer α, based on the physical mechanism, is not always possible. To overcome this difficulty what was usually done is to resort to experiment and express these results in the form of empirical correlations that can be used generally in certain situations. It has been found that the heat transfer coefficient can be related to two important dimensionless parameters in heat transfer studies, they are: Nusselt number and Prandtl number. The Nusselt number is the term used for relationship $\alpha d/\lambda$. This quantity is the ratio of heat transfer and thermal conductivity expressed by the amount λ/d. The Nusselt number can be considered a dimensionless coefficient of heat transfer. The Prandtl number is the term used for the relationship $Cp\mu/\lambda$. This is the reason between the diffusivity at the moment (as shown by the viscosity) and thermal diffusivity (expressed by the ratio of thermal conductivity and heat specific). As with the Reynolds number, a large number of works on both analytical and experimental showed the value that have the Nusselt and Prandtl numbers as parameters of heat transfer [27]. To correlate the data on heat transfer as described above, these depend mainly on the Prandtl and Reynolds numbers. The simplest relation that can be used is an exponential function for each of these parameters, so it can be assumed:

$$\mathrm{Nu} = C\,\mathrm{Re}^m\,\mathrm{Pr}^n \tag{23}$$

where C, m, and n are constants that must be determined from the experimental data. The method used to adjust the coefficients was Nelder–Mead. This method of optimization makes a minimization function which may be a multidimensional non-linear equation which also does not consider restrictions. Table 6 presents the values of the coefficients for Eq. (23). Table 7 presents the comparison of correlations proposed with empirical correlation used by [7], and it is made for the calculation of the condensation heat transfer coefficient in phase change region. The experimental data obtained with Carrol-water solution of test 1 and 2 are used.

6.2. Generation of pure water in relation to the condensate

Directly proportional behavior was observed in heat transformer water purification system to the condensed steam, similarly it is presented by Hernández et al. [28]. This was because the relationship between condensate and steam generated will make an exothermic reaction in the absorber, which leads to the purification of water. Fig. 10 shows the relationship of the condensed steam and purified water.

7. Conclusions

A helical condenser of concentric tubes coupled with a heat transformer was used to calculate the condensation coefficients of water vapor inside of the condenser tube. Heat transformer was operated with two working solutions: Carrol-water and water. Water was carried out in the range of 3.7–9.2 kPa pressure; steam Reynolds number between 6,400 and 23,500, mass flux: 10.49–39.16 kg/m²s. For the Carrol-water pressure, the range was 6.1–9.2 kPa; Reynolds number between 5,550 and 22,000, mass flux: 10.79–44.42 kg/m²s. The obtained values for the condensation coefficient presented a linear behavior in the interval from 2,400 to 6,100 W/m²℃ and 810–5,650 W/m²℃, respectively.

The similarity of the condensation coefficients obtained by energy balance and those determined by the Wilson plot method demonstrated that the method Wilson plot can be used as a tool for the calculation of the coefficients of heat transfer for helical geometry.

Obtained correlation Nusselt numbers were estimated for ranges of operation in each of the working solutions.

Carrol-water tests found that the amount of distillate in the water purification system is related to the condensed steam. An efficient condensation leads to a better control of the whole system, to a greater and constant distillation.

Nomenclature

A	—	surface (m²)
Cp	—	heat capacity (J/kg℃)
D	—	helical diameter
d	—	diameter
H	—	height of helical coils (m)
h	—	specific enthalpy (J/kg)
L	—	length (m)
LMTD	—	logarithmic mean temperature (℃)
$\dot{m}$	—	mass flow (kg/s)
Nu	—	Nusselt ($\alpha d/\lambda$)
Pr	—	Prandtl ($Cp\mu/\lambda$)
P	—	pressure (kPa)
$\dot{Q}$		heat flux (W)
Re		Reynolds ($\rho dv/\mu$)
Rov		overall thermal resistance (℃/W)
t	—	time (s)
T	—	temperature (℃)
U	—	overall heat transfer coefficient (W/m²℃)
V	—	speed (m/s)
r	—	radio (m)
$\dot{w}$	—	volumetric flow (m³/s)

Greek symbols

α	—	convective heat transfer coefficient (W/m²℃)
ΔT	—	temperature difference (℃)
λ	—	thermal conductivity (W/m℃)
μ	—	viscosity (Pa s)
ρ	—	density (kg/m³)
v	—	volume (m/s)

Subscript

ab	—	absorber
be	—	energy balance
cf	—	phase change
co	—	condenser
ev	—	evaporator
con	—	condensation
ext	—	outer
ge	—	generator
in	—	inlet
int	—	internal
ls	—	saturated liquid
out	—	output
sat	—	saturation
se	—	sub-cooling
sim	—	simulated
v	—	vapor
w	—	wall
wp	—	Wilson plot

References

[1] R.C. Xin, Natural convection heat transfer from helicoidal pipes, J. Thermophys. Heat Transfer 10 (1996) 297–302.

[2] J.A. Hernández, D. Juárez-Romero, L.I. Morales, J. Siqueiros, COP prediction for the integration of a water purification process in a heat transformer: With and without energy recycling, Desalination 219 (2008) 66–80.

[3] R.F. Escobar, D. Juárez, J. Siqueiros, C. Irles, J.A. Hernández, On-line COP estimation for waste energy recovery heat transformer by water purification process, Desalination 222 (2008) 666–672.

[4] F.A. Holland, J. Siqueiros, S. Santoyo, C.L. Heard, E.R. Santoyo, Water Purification Using Heat Pumps, first ed., E & FN Spon, 1999.

[5] W. Rivera, R. Best, J. Hernandez, C.L. Heard, F.A. Holland, Thermodynamic study of advanced absorption heat transformer I. Single and two stage configurations with heat exchangers, Heat Recovery Syst. CHP 14 (1994) 173–183.

[6] M. Balcilar, K. Aroonrat, A.S. Dalkilic, S. Wongwises, A numerical correlation development study for the determination of Nusselt numbers during boiling and condensation of R134a inside smooth and corrugated tubes, Int. Commun. Heat Mass Transfer 48 (2013) 141–148.

[7] D. Colorado, J.A. Hernandez, O. Garcia-Valladares, A. Huicochea, J. Siqueiros, Numerical simulation and experimental validation of a helical experimental validation of a helical double-pipe vertical condenser, Appl. Energy 88 (2011) 2136–2145.

[8] D. Colorado-Garrido, E. Santoyo-Castelazo, J.A. Hernández, O. García-Valladares, J. Siqueiros, D. Juarez-Romero, Heat transfer of a helical double-pipe vertical evaporator: Theoretical analysis and experimental validation, Appl. Energy 86 (2009) 1144–1153.

[9] A.S. Dalkilic, S. Wongwises, Intensive literature review of condensation inside smooth and enhanced-tubes, Int. J. Heat Mass Transfer 52 (2009) 3409–3426.

[10] A.S. Dalkilic, S. Wongwises, Book Chapter, Condensation heat transfer in smooth and enhanced geometries —A review of 2010 literature, in: Refrigeration Systems, Design Technologies and Developments, Nova Publishers, Hauppauge, NY, 2013.

[11] S. Laohalertdecha, A.S. Dalkilic, S. Wongwises, A review on the heat-transfer performance and pressure-drop characteristics of various enhanced tubes, Int. J. Air Cond. Refrig. 20 (2012) 1–20.

[12] M. Balcilar, A.S. Dalkiliç, A. Çelen, N. Kayaci, S. Wongwises, A critical review on the numerical methods of two-phase flows, ASME 2012 IMECE (2012), November 9–15, USA, 2012.

[13] R.C. Xin, A. Awwad, Z.F. Dong, M.A. Ebadian, An experimental study of single-phase and two-phase flow pressure drop in annular helicoidal pipes, Int. J. Heat Fluid Flow 18 (1997) 482–488.

[14] H.J. Kang, C.X. Lin, M.A. Ebadian, Condensation of R-134a flowing inside helicoidal pipe, Int. J. Heat Mass Transfer 43 (2000) 2553–2564.

[15] T.J. Rennie, G.S.V. Raghavan, Laminar Parallel Flow in a Tube-in-Tube Helical Heat Exchanger, the AIC 2002 Meeting CSAE/SCGR Program Saskatoon, Saskatchewan, Paper No. 02-406, 2002.

[16] S.K. Singh, R. Kumar, B. Mohanty, Heat transfer during condensation of steam over a vertical grid of horizontal integral-fin copper tubes, Appl. Therm. Eng. 21 (2001) 717–730.

[17] R. Kumar, H.K. Varma, K.N. Agrawal, B. Mohanty, A comprehensive study of modified Wilson Plot technique to determine the heat transfer coefficient during condensation of steam and R-134a over single horizontal plain and finned tubes, Heat Transfer Eng. 22 (2001) 3–12.

[18] W. Wagner, H.-J. Kretzschmar, International Steam Tables: Properties of Water and Steam Based on the Industrial Formulation IAPWS-IF97, second ed., Springer, Berlin Heidelberg, 2008.

[19] F.W. Dittus, L.M.K. Boelter, Heat Transfer in Automobile Radiators of the Tubular Type, University of California Publications in Engineering, vol. 2, 1930, pp. 443–461. Reprinted. In: Int. Commun. Heat Mass 12 (1985) 3–22.

[20] O. Garcia Valladares, Review of in tube condensation heat transfer correlations for smooth and microfin tubes, Heat Transfer Eng. 24 (2003) 6–24.

[21] M.H.R. Fazlur-Rahman, R. Devanathan, Modelling and dynamic feedback linearization of a heat exchanger model, in: Proceedings of the Third IEEE Conference on Control Applications, 3, 1994, pp. 1801–1806.

[22] E. Weyer, G. Szederkényi, K. Hangos, Grey box fault detection of heat exchangers, Control Eng. Pract. 8 (2000) 121–131.

[23] E.I. Varga, K.M. Hangos, F. Szigeti, Controllability and observability of heat exchanger networks in the time-varying parameter case, Control Eng. Pract. 3 (1995) 1409–1419.

[24] A.W. Alsop, T.F. Edgar, Nonlinear heat exchanger control through the use of partially linearized control variables, Chem. Eng. Commun. 75 (1989) 155–170.

[25] P.J. Marto, An evaluation of film condensation on horizontal integral-fin tubes, J. Heat Transfer 110 (1988) 1287–1305.

[26] Z. Berk, Food Process Engineering and Technology, second ed., International Series, Elsevier, London, 2013.

[27] B.S. Petukhov, Heat transfer and friction in turbulent pipe flow with variable physical properties, Adv. Heat Transfer 6 (1970) 503–564.

[28] J.A. Hernández, D. Colorado, Uncertainty analysis of COP prediction in a water purification system integrated into a heat transformer using several artificial neural networks, Desalin. Water Treat. 51(7–9) (2013) 1443–1456.